

# Nitride-based semiconductors for blue and green light-emitting devices

F. A. Ponce & D. P. Bour

**Recent advances in fabrication technologies for the semiconducting nitrides of the group III elements have led to commercially available, high-efficiency solid-state devices that emit green and blue light. Light-emitting diodes based on these materials should find applications in flat-panel displays, and blue and ultraviolet laser diodes promise high-density optical data storage and high-resolution printing.**

The production of light has been of paramount importance to humankind since the dawn of civilization. From the use of fire to the incandescent electric lamp, the evolution of lighting technology has been characterized by the invention of increasingly brighter and more efficient light sources. The incandescent electric lamp was first demonstrated by Thomas Edison in 1879, and with the introduction of thin tungsten wire filaments at the turn of the century, light-bulb manufacture became a major industry. More powerful and efficient light sources followed, such as the neon lamps at the beginning of the century and the fluorescent tube in 1930. By the 1950s, the methods of lighting seemed well established, with filament and fluorescent lamps for interiors, neon lamps for exterior advertising and signs, and sodium discharge lamps for streets<sup>1</sup>.

Electronic lighting technology made its appearance with the advent of semiconductors during the second part of the twentieth century. The achievement of high-efficiency electroluminescence from semiconductor devices in early 1962 led to light-emitting-diode (LED) technology<sup>2</sup>. Later in the same year, light amplification by stimulated emission (laser action) in a semiconductor was demonstrated by four groups<sup>3,4</sup>. Initially restricted to red light, and later extended to yellow, LEDs were first used in wrist watches and instrument panel indicators. The development of semiconductor diode lasers allowed the production of highly coherent bright light emitters that soon found applications in telecommunications (optical fibre networks), data storage (compact-disk technology), and document production (laser printers). LEDs operating in the red-to-yellow portion of the spectrum, with light emission efficiencies superior to those of incandescent lamps, became available in the early 1990s<sup>5,6</sup>.

But it has proved difficult to extend these light sources into the short-wavelength region of the spectrum, from green to violet. Weak blue LEDs made from semiconducting SiC have been fabricated, but they are orders of magnitude less efficient than their red and yellow counterparts. The II-VI semiconducting compounds, especially those based on ZnSe, have shown some promise as blue and green light sources; but the facile formation of structural defects diminishes their lifetime and their potential usefulness for commercial applications. Much research has been done in the past three decades on the group III nitrides, comprising the Al-Ga-In-N alloys, which have the characteristic wide bandgap necessary for short-wavelength visible-light emission<sup>7-10</sup>. In recent years research on nitride semiconductors has suddenly yielded dramatic advances, culminating in 1994 with the commercial introduction of extremely bright LEDs based on gallium nitride and operating in the green-to-ultraviolet range, with efficiencies superior to those of incandescent lamps and comparable to red and yellow LEDs. And these materials have now also been used in diode lasers operating at room temperature and emitting light in the blue-violet range, first

under pulsed conditions<sup>11</sup> in late 1995 and very recently under continuous operation<sup>12</sup>.

With these technological advances, two particularly important areas of application are opened up. One is the ability to produce all three primary colours in LEDs, which implies applications in traffic lights, outdoor signs and large panel displays (see Box 1). The other is the availability of shorter-wavelength diode lasers, with the ability to project coherent radiation and to focus laser light into smaller spots (in the optical diffraction limit, the size of a focused spot is proportional to the wavelength of the light). This raises the possibility of high-density optical information storage and read-out. Green-to-ultraviolet lasers also bring closer to reality technologies such as full-colour photographic film printers, high-resolution laser printing, and projection television using full colour diode laser sources. Nitride semiconductors now look well placed to bring these possibilities to fruition.

## The light-emitting diode

The light-emitting diode is the basic component for electronic lighting technology. It is a relatively simple semiconductor device that emits light when an electric current is passed through it. It consists of a back-to-back sandwich of p-type and n-type semiconductor materials (a p-n junction) characterized by a bandgap

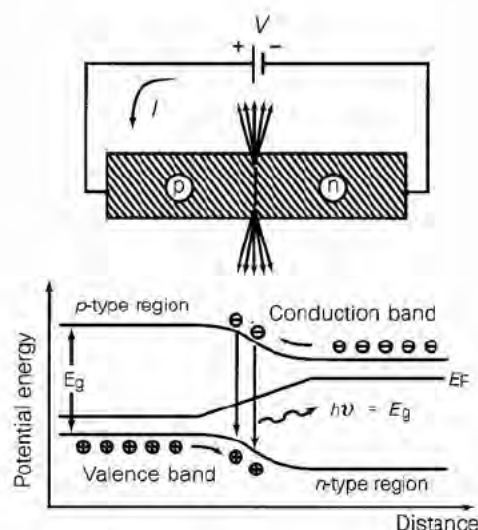


**Figure 1** Schematic diagram of a light-emitting diode. The characteristics of the emitted light are related to the energy gap  $E_g$  between the conduction and valence band in the semiconductor.  $E_F$  is the Fermi energy.



## Box 1 Achieving full-colour displays

The relevance and impact of the recent achievements in the III-V nitrides can be understood via the chromaticity diagram (see figure), which shows the relationship between the colours we see<sup>57,58</sup>. The basis for the chromaticity diagram is the spectral sensitivity of the three types of cones in the human eye. Colorimetry therefore represents every colour by three parameters, corresponding to the output of each type of cone. As an example of how different colour mixtures can produce the same colour response, white light can be perceived in a number of ways. In one case, it may comprise a continuous spectrum of all visible wavelengths, as in the black-body emission from the Sun or an incandescent bulb. Alternatively, it may contain a series of more discrete spectral lines, for example as in the blue and yellow emissions from a fluorescent lamp. Although all these source colours appear white to the eye, their spectral compositions are substantially different.

The theoretical foundation of the chromaticity diagram is simply that any colour can be created by mixing three primary colours. Using a standardized set of primaries, the chromaticity diagram thus shows the amounts of each primary colour required to create another colour. The horizontal and vertical axes of the chromaticity diagram thus represent the fractions of two of the primaries. As the percentages of each of the three primary colours in the mixture must add to 100%, the fraction corresponding to the third primary is uniquely determined by specifying the other two. When the (*x*, *y*) coordinates of a point on the chromaticity are given, these correspond to the fractions of two primaries (with the remainder equivalent to the fraction of the third primary). Hence, the chromaticity diagram can show the colour of this particular combination, or any other combination, in a two-dimensional plot.

Any light source such as an LED, laser or lamp can be represented by a single point on the chromaticity diagram. Spectrally pure, monochromatic sources (such as a laser) are represented by points along the outer perimeter of the diagram. In this situation, when the peak wavelength (shown around the perimeter) and spectral width of such an emitter is specified, its coordinates on the chromaticity diagram are similarly determined. For instance, the coordinates of a pure blue emitter lie on the bottom left corner of the diagram (point 2). This corresponds to Nichia's super-bright blue InGaN LEDs. The output of pure red AlGaAs LEDs is identified by point 1.

When the spectral width of a source increases, and the emission is therefore less pure, the colour coordinates move towards the central (white) region of the diagram. This is indicated by point 3, which specifies Nichia's green 520 nm emission from an InGaN LED. Here, the spectral width is about 40 nm, or twice that of the blue LED. Consequently, the colour coordinate is displaced more from the perimeter of the chromaticity diagram. An extreme case of a spectrally broad emission spectrum is the black-body radiation associated with a body heated to about 10,000 K, which would appear white. This emission would be represented by a point in the central, white region of the chromaticity diagram, because this broadband emission is equivalent to a roughly equal mixture of all three primaries.

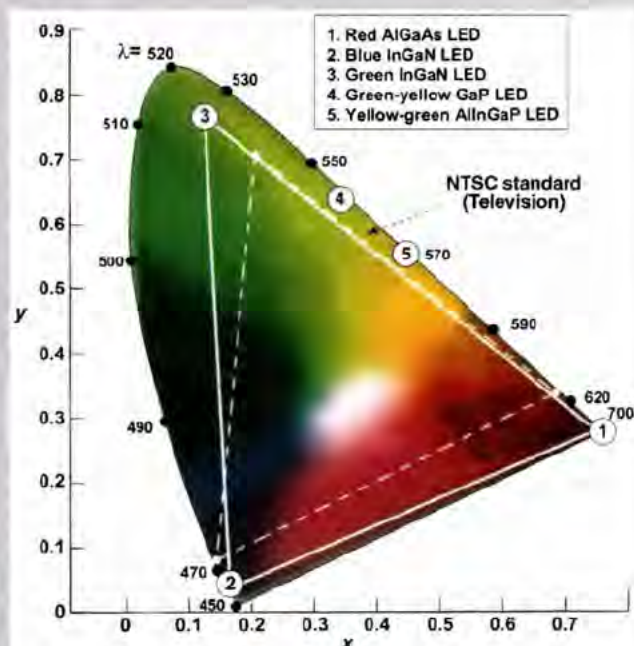
The chromaticity diagram also illustrates how two (or more) pure colours may be mixed to form an infinite palette of intermediate colours. Consider the case of a commercial red LED (point 1) and a green LED (point 3). When these two sources are combined, any colour on the line connecting them can be reproduced. For example, starting from the red colour specified by point 1, as a small amount of the green is mixed in, the colour will become orange. When the component red and green intensities are roughly equal (or midway between points 1 and 3), the colour of the mixed source is perceived as yellow. In a similar manner, yellow light may be combined with complementary blue light, to produce white. In fact, this combination of complementary yellow and blue colours is one approach to making solid-state white lamps; using a blue LED to excite phosphors is another alternative.

Similarly, when three sources are specified, they may be combined to produce all the colours contained within the triangular area defined by their coordinates on the chromaticity diagram. For example, the commercial red (point 1), green (point 3), and blue (point 2) LEDs may be combined to produce all the colours defined by the triangle shown. This demonstrates why the

recent development of bright blue and green emitters (taken with the pre-existing red LEDs) is so important. Using the pure red, green and blue emitters as primaries, nearly the entire chromaticity diagram is spanned. In other words, these three colours can be combined to generate nearly all colours, and so they form a minimum set of three sources which can be used to produce a true full-colour display. For comparison, the NTSC colour television standard based on luminescence from phosphor-coated cathode ray tubes is shown in the dashed triangle. From the figure it is observed that full-colour LEDs can provide a broader range of colours than those available on television screens.

Before 1994, only a narrow segment (yellow-green to red, or wavelength from 555 to 700 nm) of the colour diagram was accessible with high-efficiency LEDs. Although blue SiC LEDs were available before this, their efficiency was rather low, restricting their application. An optimum green wavelength of 520 nm was also not possible. The best green sources were in fact a yellow-green, fabricated from either nitrogen-doped GaP (point 4) or AlGaInP (point 3), a semiconductor alloy whose compositions can be adjusted to produce red, orange or yellow emission. Although AlGaInP is used to make the world's most efficient LEDs, which are yellow, it could not be extended to a shorter, green wavelength because it becomes an indirect bandgap semiconductor.

Today, most colours can not be produced by combining the red GaAlAs LEDs with the green and blue InGaN LEDs in a single full-colour LED lamp. In such a package, a sophisticated electronic controller adjusts the current to each LED, so that the combination of the red, green and blue outputs produces any desired colour. Similarly, when the nitride LEDs are evolved into green and blue semiconductor lasers, they could be combined with existing red lasers to create projection displays and colour film printers.



**Box figure** Chromaticity diagram from CIE (Commission Internationale de l'Éclairage) 1931. The monochromatic colours appear on the arch and their wavelength is indicated in nm. White light is located near the centre of the diagram. The colours of commercially available LEDs are shown. Note that the green and blue InGaN in combination with the red GaAlAs LEDs cover a large section of the chromaticity diagram, giving purer colour than the NTSC television standard (depicted by the dashed triangle). Colour range obtained from Photo Research Corporation, Chatsworth, California



$E_g$ . This quantity determines the minimum energy required to excite an electron from the valence band to the conduction band (where it is mobile). Conversely, the bandgap also determines the energy of a photon produced when a conduction electron recombines with a hole in the valence band. When a current is passed through the diode, electrons in the conduction band flow across the junction from the n-doped side, and holes in the valence band flow from the p-doped side (Fig. 1). The result is that a significant number of electrons and holes recombine at the p-n junction, emitting light with an energy  $h\nu \approx E_g$ . A direct radiative transition involves only the emission of a photon, whereas an indirect transition requires a combination of a photon and a phonon (lattice vibration). Because of the required phonon interaction, the transition probability for a material with an indirect bandgap is usually much lower than in the case of a direct bandgap. The values of  $E_g$  for semiconductors emitting in the visible range of the spectrum are shown in Fig. 2 as a function of the interatomic bond length, which exerts a primary influence on the bandgap. The value of this lattice constant is critical for film fabrication technologies, as explained later.

All commercially available LEDs in the visible-to-infrared range (about 450–1,500 nm) are made of III–V compound semiconductor thin films, consisting of elements belonging to group III (aluminum, gallium and indium) and group V (nitrogen, phosphorus and arsenic) of the periodic table. Film deposition is achieved by vapour-phase techniques involving chemical reactions that produce thin films whose lattice structures are related to that of the substrate on which they are deposited (epitaxial growth). Red LEDs made from  $\text{GaAs}_{1-x}\text{P}_x$  epitaxial layers were first introduced commercially by General Electric in 1962, following the work of Holonyak and Bevacqua<sup>3</sup>, and similar devices are still used today for low-intensity light applications. The evolution of LED performance is depicted in Fig. 3. Shorter-wavelength light emission requires a higher phosphorus content. However, for  $x > 0.45$ ,  $\text{GaAs}_{1-x}\text{P}_x$  has an indirect bandgap, causing the emission efficiency to drop

significantly. In the mid 1970s the introduction of nitrogen as a dopant enhanced the emission efficiency of  $\text{GaAs}_{1-x}\text{P}_x$  LEDs by inducing a direct bandgap behaviour. Consequently, the performance of red LEDs was improved, and orange, yellow and green light emission became possible (the latter by nitrogen doping of GaP). But the light emission efficiencies of these LEDs were inferior to those of incandescent tungsten filament lamps, which, emitting at  $\sim 20$  lumens per watt, have served as a point of reference for the performance of LEDs. (A lumen is the luminous flux intensity per solid angle of a point source with luminous intensity of one candela (cd).)

In the early 1980s, heterostructures involving junctions between materials with different bandgaps were introduced. In the late 1980s, double heterostructures (DHs), involving a smaller-bandgap semiconductor sandwiched by materials with larger bandgaps, increased the light-emission efficiency by improving electronic carrier confinement. As a result, red-emitting DH AlGaAs devices surpassed the performance of red-filtered incandescent lamps. Another order of magnitude improvement was achieved in the early 1990s with the introduction of red, orange and yellow LEDs based on AlInGaP (ref. 13). In the short-wavelength range, SiC blue LEDs also became available, but with much lower efficiencies; and work on II–VI compounds such as ZnSe was pursued intensively, aimed at developing brighter blue LEDs with sufficient durability for commercialization. The evolution of LEDs took a dramatic turn in late 1993, with the introduction by Shuji Nakamura of Nichia Chemical of highly efficient blue light emitters based on the group III nitride compounds. They were shortly followed by devices emitting in the green-to-violet range of the spectrum. This technology was made possible by persistent pioneering research over more than 20 years by Isamu Akasaki at Nagoya University (now at Meijo University). As a result, LEDs are available today covering all the primary colours of the spectrum, at competitive prices, and with energy efficiencies greater than those obtained from incandescent

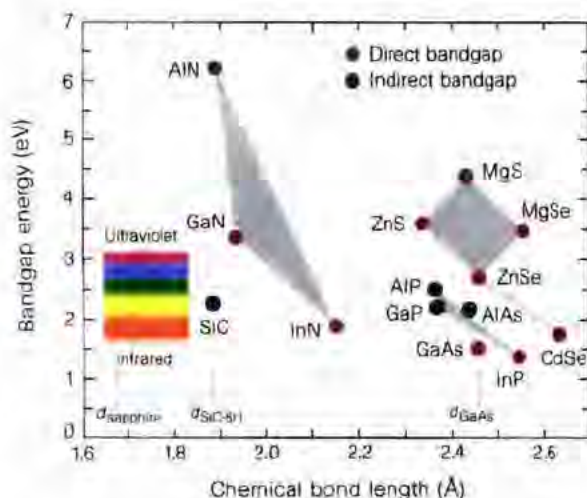


**Figure 2** Bandgap and chemical bond lengths ( $a$ ) of compound semiconductors that emit in the visible range of the electromagnetic spectrum. The visible spectrum is shown as related to the energy gap of the semiconductor. A direct-bandgap material involves only the emission of a photon per radiative event, whereas an indirect-bandgap material has radiative transitions involving a combination of a photon and a phonon (lattice vibration). The chemical bond length or interatomic separation is shown here, instead of the lattice parameter, to allow proper comparison of the hexagonal (wurtzite) nitrides with the cubic (zincblende) phosphides and arsenides. Also shown are the respective interatomic distances for relevant substrates (sapphire, SiC and GaAs).

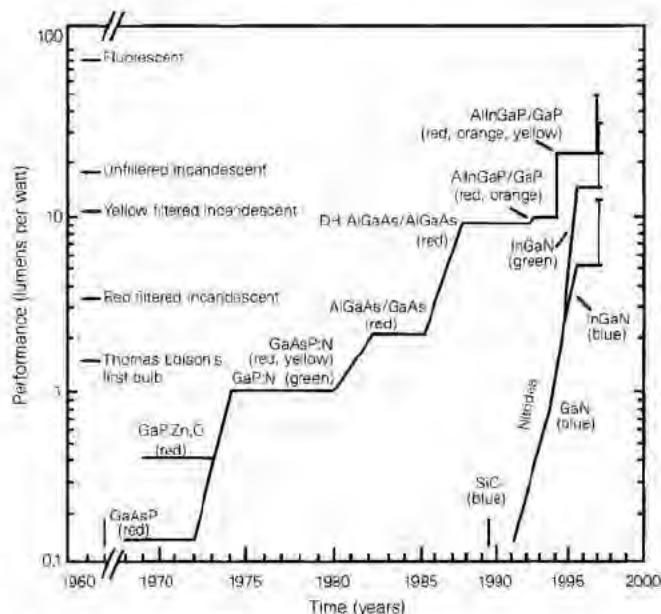


**Figure 3** Evolution of visible LEDs. Over the past three decades, the arsenides and phosphides have produced increasingly brighter LEDs in the red-to-yellow range of the visible spectrum. In the past three years the nitrides have taken over the green-to-blue range. A lumen is the luminous flux intensity within unit solid angle of a point source with luminous intensity of one candela. An incandescent tungsten filament lamp emits about 20 lumens per watt. The bars for present day correspond to production (lower end) and laboratory (upper end) performance. (Updated version from report in ref. 5.)

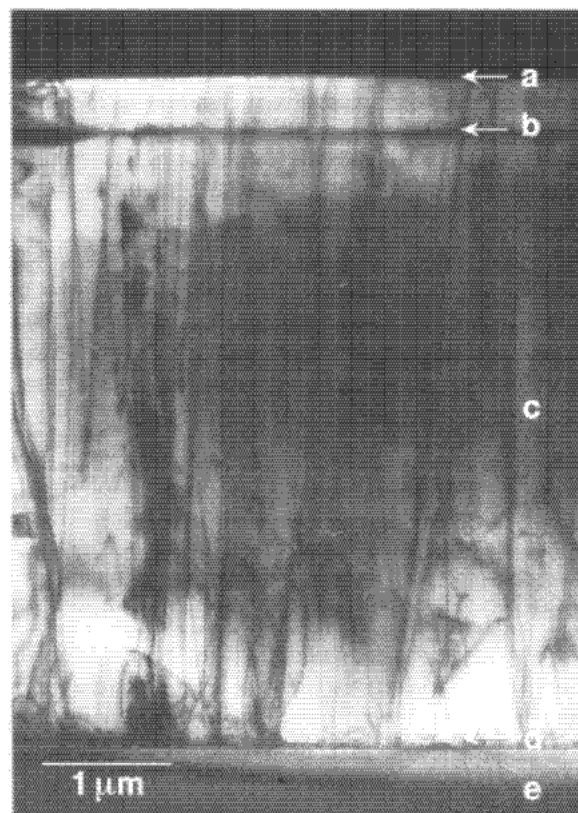


**Figure 4** Cross-section transmission electron microscopy view of a high-efficiency Nichia blue LED. The dislocation density of  $10^{10} \text{ cm}^{-2}$  is remarkably high for such an efficient and durable device. Indicated in the figure are the top surface of the film (a), the active region (b), the main GaN film (c), the buffer layer (d), and the sapphire substrate (e).

tungsten-filament lamps.

### The III-V nitrides

There are two fundamental reasons to choose nitrides for blue-light sources. Foremost is the large bandgap associated with the Al–Ga–In–N system, which encompasses the entire visible spectrum (Fig. 2). The  $\text{Ga}_x\text{In}_{1-x}\text{N}$  ternary alloys, represented in the figure by the lower segment of the nitride triangle, have bandgaps ranging from 1.9 eV (red) for InN to 3.4 eV (ultraviolet) for GaN. The other main advantage of the nitrides over other high-bandgap semiconductors is the strong chemical bond which makes the material very stable and resistant to degradation under conditions of high electric currents and intense light illumination (as encountered in the active regions of the device). The strong chemical bonds account also for the difficulty in introducing dislocations once the material is grown, thus removing one of the main mechanisms of degradation observed in other III–V compounds.

Among the obvious disadvantages of the nitrides is the apparent absence of suitable substrates for film growth; the high growth temperatures made necessary by the strong chemical bonding in these materials limit the choice of substrates to those that are stable at such elevated temperatures. The two most commonly used are sapphire ( $\alpha\text{-Al}_2\text{O}_3$ ) and silicon carbide (6H-SiC). The large differences in lattice parameter and in linear thermal expansion rates that occur both within the AlGaInN system itself and relative to these substrates meant that poor-quality epitaxial films were expected. The microstructure of films grown on sapphire, however, appears to have special properties that overcome these obstacles, as discussed later.

The III–V nitrides are not really new materials. AlN was reported in 1907 (ref. 14), and it is believed to be one of the first III–V compound semiconductors ever synthesized. The crystalline structure of GaN was described in 1937 (ref. 15) and growth of GaN crystalline films was reported in 1969 (ref. 16). Three important milestones were achieved in 1971. First, Pankove<sup>17</sup> reported metal–

**Table 1** Development of group III nitrides

Year	Event	Authors	Reference
1969	GaN by hydride vapour phase epitaxy	Maruska and Tietjen	16
1971	Metal–insulator–semiconductor LEDs	Pankove <i>et al.</i>	17
	GaN by MOCVD	Manasevit <i>et al.</i>	18
	Ultraviolet stimulated emission at 2 K	Dingle <i>et al.</i>	19
1974	GaN by sublimation	Matsumoto and Aoki	51
	GaN by MBE	Akasaki and Hayashi	52
1975	AlN by reactive evaporation	Yoshida <i>et al.</i>	53
1982	Synthesis (high pressure)	Karpinski <i>et al.</i>	54
1983	AlN intermediate layer (MBE)	Yoshida <i>et al.</i>	20
1986	Specular films using AlN buffer layers	Amano <i>et al.</i>	23
1989	p-type doping with Mg and LEEBI	Amano <i>et al.</i>	26
	GaN p–n junction LED	Amano and Akasaki	26
	InGaIn epitaxy (XRR = 100 arcmin)	Nagamoto <i>et al.</i>	55
1991	GaN buffer layer by MOCVD	Nakamura <i>et al.</i>	37
1992	Mg activation by thermal annealing	Nakamura <i>et al.</i>	27
	High-brightness AlGaIn ultraviolet/blue LED (1.5%)	Akasaki and Amano	28
	InGaIn epitaxy (XRR = 5 arcmin)	Nakamura <i>et al.</i>	56
	High-brightness AlGaIn ultraviolet LEDs	Akasaki <i>et al.</i>	28
1993	InGaIn MQW structure	Nakamura <i>et al.</i>	29
	InGaIn/AlGaIn DH blue LEDs (1 cd)	Nakamura <i>et al.</i>	30
	InGaIn/AlGaIn DH blue-green LEDs (2 cd)	Nakamura <i>et al.</i>	31
1995	InGaIn QW blue, green and yellow LEDs	Nakamura <i>et al.</i>	33
	InGaIn SQW green LEDs (10 cd)	Nakamura <i>et al.</i>	34
	Blue laser diode, pulsed operation	Nakamura <i>et al.</i>	11
1996	Ultraviolet laser diode	Akasaki <i>et al.</i>	49
	Blue laser diode, pulsed operation	Itaya <i>et al.</i>	50
	Blue laser diode, c.w. operation	Nakamura <i>et al.</i>	12

Key steps in the development of the group III nitrides are listed with respective authors and references. The following abbreviations are used: low-energy electron beam irradiation (LEEBI), X-ray rocking curves (XRR), multiple quantum wells (MQW), quantum well (QW), single quantum well (SQW), double heterostructure (DH), continuous wave (c.w.).



insulator–semiconductor LEDs made of GaN thin films. Manasevit<sup>18</sup> succeeded in growing GaN by the technique of metal-organic chemical vapour deposition (MOCVD) for the first time, using a method that is still used today. Finally, GaN needles were grown by Dingle<sup>19</sup>, who also reported stimulated light emission from this material at a temperature of 2 K, establishing the prospect of ultraviolet semiconductor injection lasers. The key developments during the following years are summarized in Table 1. The main obstacles to be overcome in making practical nitride-based devices involved difficulties in growing smooth films, in controlling n-type conductivity, in producing p-type materials and in growing AlGaIn and InGaIn alloys. Initial films were typically rough and fractured, features attributed to three-dimensional nucleation (a two-dimensional growth mode is required to produce smooth films) and the choice of substrates. These obstacles appeared insurmountable for many years, so the nitrides were largely ignored in favour of other large-bandgap materials.

Mastering epitaxy on foreign substrates is considered necessary to control the chemical purity of a semiconductor such as GaN, thus avoiding unwanted impurities which influence the optical and electronic character of the material. Similarly, during epitaxial growth it is desirable to minimize structural imperfections in the lattice such as dislocations and stacking faults, which are known to have adverse effects on optoelectronic properties of semiconducting materials (such as the quantum efficiency associated with light emission). In the search for improved properties, Yoshida<sup>20</sup> showed that an AlN intermediate layer between a sapphire substrate and an epitaxial GaN film increases the efficiency of cathodoluminescence (luminescence excited by a high-energy electron beam) of the films. Parallel developments, in particular in GaAs epitaxy on silicon<sup>21,22</sup>, demonstrated that smooth epitaxial thin films on substrates with a large (> 4%) lattice mismatch could be achieved by the initial deposition of low-temperature nucleation (or buffer) layers. Although amorphous and therefore not of as high quality as the desired film, the buffer layers allowed for continuous coverage of the substrate and overcame the wetting obstacles related to surface and interface energetics. Using AlN low-temperature buffer layers on sapphire substrates, Akasaki and Amano<sup>23</sup> grew the first smooth surfaces of GaN films in 1986, demonstrating that two-dimensional nucleation in nitride epitaxy could be achieved and thereby bringing about a significant improvement in the electrical and luminescent properties of the films. Akasaki *et al.*<sup>23</sup> also demonstrated that silane (SiH<sub>4</sub>) could be used for effective and controllable n-type doping.

Making p-type GaN films took a few more years. Magnesium was expected to be a good acceptor (p-type dopant); but although it was possible to incorporate significant concentrations of Mg in GaN, it did not effectively introduce hole charge carriers—the films were highly resistive. Similar observations in other materials such as GaAs and InP had established that unintentional hydrogen contamination played a strong role in passivating p-type dopants<sup>24,25</sup>. In 1989, Amano and Akasaki demonstrated that low-energy electron-beam irradiation (LEEBI) activated magnesium-doped GaN films<sup>26</sup>, converting them from a highly resistive state to one having a high ( $\sim 10^{16}$  cm<sup>-3</sup>) concentration of holes. This p-type carrier density was sufficient to produce the first p–n junction blue LEDs<sup>26</sup>. In 1992, Nakamura showed that superior hole concentrations could be achieved by thermal annealing after growth<sup>27</sup>. These developments set the stage for brighter LEDs by Akasaki, Amano and others in 1992 (ref. 28). The development of extremely thin (quantum-well) layers of indium-rich nitrides by Nakamura brought increasingly superior performance<sup>29,30</sup>, culminating with the announcement by Nichia Chemical Industries in November 1993 of the development of a bright blue LED and plans for mass production.

### Blue and green LEDs

The first blue LEDs based on the III–V nitrides were made commercially available by Nichia in early 1994. They consisted of

an InGaIn/AlGaIn double heterostructure, fabricated by codoping Zn and Si into the InGaIn active layer<sup>30</sup>. The output power was 3 mW at a forward current of 20 mA, with an external quantum efficiency (ratio of photons produced to the number of injected electrons) of 5.4% and a peak wavelength of 450 nm. Shortly thereafter, blue–green LEDs were fabricated by increasing the indium concentration in the InGaIn active layer, yielding a brightness of 2 cd (ref. 31).

Most surprising was that, compared with LEDs fabricated using other semiconductors, the light-emitting efficiencies of these GaN-based LEDs were remarkably insensitive to extended lattice defects such as dislocations in the films. Transmission electron microscopy (TEM) studies<sup>32</sup> indicated that the material contained  $10^{10}$  dislocations per square centimetre, more than six orders of magnitude above any other material used for LED fabrication. Figure 4 shows such a TEM cross-section image of a bright blue Nichia LED. Dislocations run in the growth direction (vertical), their density does not vary with distance from the sapphire interface, and they traverse the active region of the device. The fact that efficient GaN-based LEDs can be made despite such high densities of structural defects indicates a critical difference between the group III nitrides and other semiconductors.

Devices with longer peak emission wavelengths have been fabricated using extremely thin InGaIn layers (quantum wells) containing high concentrations of indium; these materials access the green and yellow range of the visible spectrum<sup>33</sup>. In addition to producing longer wavelengths, quantum wells also narrow the spectral width of the emitted light, compared with the impurity-related transitions of the earlier DH LEDs, improving the monochromaticity. Bright green InGaIn single-quantum-well (SQW) LEDs have now been produced with an output power of 3 mW at a forward current of 20 mA, with a luminous intensity of 10 cd, an external quantum efficiency of 6.3%, and a peak wavelength of 520 nm (ref. 34). The green colour of the emitted light is much 'deeper' (more monochromatic) than that available from conventional GaP and AlInGaP, and the intensity is about 100 times higher.

Data on the reliability and lifetime of these devices are still limited. Long lifetimes have been reported, most in excess of 50,000 hours (lifetimes of  $\sim 10^6$  hours > 100 years have been estimated S. Nakamura, personal communication), and there is no record of observed degradation mechanisms in the nitrides. Some reports even indicate that the material itself becomes more efficient with time, and that lamp failure is due to breakdown of the contacts or of the encapsulant but not of the semiconductor itself.

### Growth and characteristics of the III–V nitrides

Several techniques, such as hydride vapour-phase epitaxy and molecular-beam epitaxy, have been successful in producing high-quality III–V nitride thin films. But as with other III–V compounds, MOCVD is the method of choice for commercial applications. The design of the growth reactor varies from vertical to horizontal flow configurations, and various gas sources have been used. The most commonly used gas-source precursors are trimethyl gallium (Ga(CH<sub>3</sub>)<sub>3</sub>) and ammonia (NH<sub>3</sub>). Likewise, InGaIn and AlGaIn can be grown by the addition of trimethyl indium and trimethyl aluminum, respectively. Typical growth techniques today involve growth on [0001] sapphire substrates, with a low-temperature AlN or GaN buffer layer of thickness 10–40 nm deposited at about 550 °C. This is followed by GaN epitaxy at 700–1,100 °C. The initial buffer layer is amorphous and undergoes solid-phase crystallization during the heating step prior to epitaxy. TEM images of the substrate/buffer layer region (Fig. 5a) indicate an abrupt crystalline transition between the two lattices<sup>35</sup>. The lack of coherence (continuity) between the sapphire and the nitride is also apparent; high-quality epitaxy is evidently achieved without such one-to-one correspondence between the crystalline lattices. Slight variations in the orientation of the epitaxial GaN layer are accommodated by

dislocations. This results in a columnar structure consisting of single crystal domains with diameters of under one micrometre, and with a distribution in lattice orientation (columnar tilt or twist) of about 5 arcmin. Spatially inhomogeneous cathodoluminescence correlates well with the columnar structure and the distribution of dislocations in the material, indicating a connection between microstructure and light emission<sup>36</sup>. This microstructure results in high-quality GaN films exhibiting smooth surface morphologies and electron mobilities of about  $600 \text{ cm}^2 \text{ V}^{-1} \text{ s}^{-1}$  at room temperature<sup>33,37</sup>. The carrier concentration of n-type GaN films can be controlled between  $1 \times 10^{17} \text{ cm}^{-3}$  and  $2 \times 10^{19} \text{ cm}^{-3}$  using silicon as dopant<sup>37</sup>. Similarly, using magnesium and activating the doping process by thermal annealing<sup>27</sup>, p-type GaN can be produced with hole concentrations of the order of  $1 \times 10^{18} \text{ cm}^{-3}$ .

In addition to sapphire, silicon carbide is also used for the growth of the nitrides. The lattice structure, interatomic separation and thermal expansion rates of the nitrides are much more similar to those of SiC than to those of sapphire<sup>38,39</sup>. These close similarities produce highly coherent changes in the atomic arrangement between SiC and the nitrides, as seen in lattice images of the interface between these two materials (Fig. 5b). In view of these similarities, it is surprising that so far devices fabricated from nitride epitaxy on SiC have inferior properties to those deposited on sapphire. One possible explanation may be the difficulty of preparing atomically flat SiC surfaces. Another is that dislocations do not compromise the performance of the materials; indeed, they even appear to be beneficial, by providing local-strain relaxation mechanisms which allow high optoelectronic performance. Epitaxy on bulk GaN single crystals has been demonstrated<sup>40</sup>, with dislocation densities below  $10^6 \text{ cm}^{-2}$ . The poor availability of sufficiently large GaN single crystals, however, limits the practicality of this choice of substrate.

## Diode lasers

The main focus of research on III-V nitrides is now the realization of a current-injected laser diode that can be operated under continuous-wave (c.w.) conditions at room temperature. Optically pumped stimulated emission has been reported in GaN (refs 41, 42), InGaN (refs 43, 44), AlGaIn/InGaIn double heterostructures<sup>45</sup>, and GaN/AlGaIn double heterostructures<sup>46</sup>. But despite the

established success of nitride LEDs by 1995, there was still much uncertainty concerning the feasibility of injection lasers. In particular, it was not clear that material with such a heavily faulted crystal structure could survive the extremely high current density required for generating optical gain in a laser, roughly two orders of magnitude greater than LED current. In late 1995 and early 1996, however, Nakamura demonstrated violet-blue injection laser action in InGaIn/GaN/AlGaIn-based heterostructures under pulsed conditions on {0001} and {11 $\bar{2}$ 0} sapphire substrates<sup>11,47</sup> (Fig. 6).

A laser diode differs from an LED in that it must provide optical gain, guide the emitted photons and also incorporate a resonant cavity for feedback. The layer stack that makes up a laser diode structure (Fig. 7) is thus more sophisticated than that of an LED, as it must accomplish these several additional functions. As in an LED (Fig. 1), the heterostructure must energetically confine injected carriers into an active region. But because lasers operate at much higher current densities than LEDs, greater confinement is required. The laser heterostructure also forms a slab waveguide, designed to concentrate the optical mode over the p-n junction (active region) in order to maximize the optical gain.

In a semiconductor, optical gain is realized when a high population of electrons and holes is injected into the active region. The lasing threshold is reached when the optical gain is sufficient to overcome all the optical losses. Pumping mechanisms for semiconductor lasers include optical- and electron-beam excitation, or, in the case of a laser diode, carrier injection across a p-n junction. Accordingly, the active region of a laser diode is located precisely at the p-n junction, so that when the diode is forward biased, the charge carriers are injected into the active region. Because the active region has a smaller bandgap than the surrounding layers, the electrons and holes are energetically confined to this region; and because of its small dimensions, a high injected carrier density is more easily achieved.

The active layer of high-performance devices are typically ultra-thin (20–50 Å) layers. Such layers are called quantum wells, because their width is less than the de Broglie wavelength of a conduction electron. This space quantization in one dimension gives rise to several beneficial effects. First, the available electron states become quantized, leading to an overall reduction in the density of states,

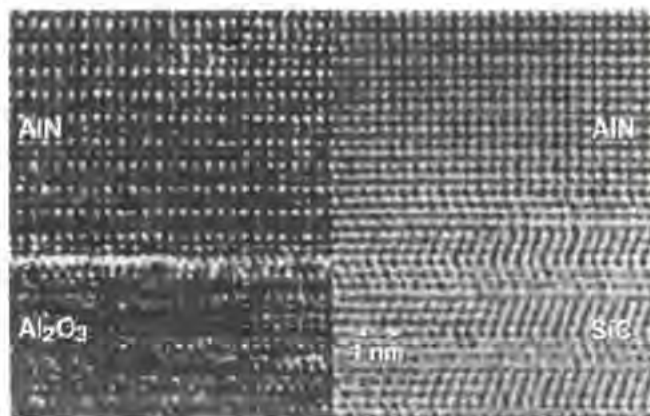


**Figure 5** Atomic arrangement at the substrate/nitride interface is critical for high-quality material. Left, nitrides grown on sapphire are epitaxial in spite of the large difference in lattice parameter and crystalline structure. Right, nitride epitaxy on SiC is characterized by coherent interfaces due to the similarity between the lattice structures. In both cases the interfaces are atomically flat and abrupt, indicative of the stability and ease of growth of these materials.



**Figure 6** Laser diode operating under pulsed current injection of 1.4 A at room temperature<sup>47</sup> (courtesy of S. Nakamura, Nichia).



thereby requiring that fewer carriers be injected to reach optical gain. Second, the quantization influences the electron and hole wavefunctions, thereby making the gain anisotropic with respect to polarization. This anisotropy favours one polarization over the other, with a consequent increase in optical gain. For these reasons, a quantum-well (or multiple-quantum-well) active region is superior to a thicker active region, which behaves more like a bulk material.

In a semiconductor laser, a resonant cavity is typically realized by cleaving end-facets on a laser diode and relying on reflection from these facets. Because the entire wafer and epitaxial layers form a single crystal, the facets are thus guaranteed to be perfectly parallel and vertical. Unfortunately, the cleavage planes of GaN and sapphire are not necessarily aligned, making cleaved facets difficult. Consequently, the formation of a resonant cavity is difficult for nitrides. Whereas the first nitride laser had very rough, plasma-etched facets, recently they have been formed by more traditional cleaving<sup>47</sup>. In this case, cleaved facets were possible because the layers were grown on {1120} sapphire rather than {0001} substrates: this makes the cleavage planes of the GaN and sapphire nearly aligned and perpendicular to the growth plane.

The threshold current density of nitride lasers is still very high; the best reported values<sup>18</sup> are about  $3,000 \text{ A cm}^{-2}$ , more than an order of magnitude higher than those of red and infrared laser diodes. This, coupled with their relatively high electrical resistance, makes heat generation a problem. Lower thresholds are likely, however, as the layer structures and resonators are optimized. For example, the first nitride injection laser had an active region containing 26 InGaN quantum wells, each being only 25 Å thick and separated by 75-Å barriers<sup>11</sup>. Although the requirement for multiple quantum wells might be aimed at achieving sufficient optical gain, this was still an unusually high number of quantum wells. Nevertheless, since this first demonstration, Nakamura's structures have evolved towards fewer (3–5) quantum wells and better-quality facets<sup>48</sup>. Likewise, Akasaki has produced a single-quantum-well laser that operates in the ultraviolet<sup>49</sup>. Also notable is the demonstration of a pulsed nitride laser by Itaya *et al.* at Toshiba<sup>50</sup>. The most impressive achievement so far, in late 1996, is Nakamura's operation of a nitride laser continuously at room temperature for 35 hours, under a constant output power of 1.5 mW per facet, with operating currents in the range of 100–280 mA (ref. 12).

InGaN segregation may play a critical role in the mechanism by

which optical gain is produced in the nitrides. When the InGaN alloy becomes unstable and separates into regions of different compositions, the regions of high-indium content tend to confine injected carriers, as a consequence of their lower bandgap energy. Thus, the InGaN segregation may lead to the formation of quantum dots, providing space quantization in three dimensions. Furthermore, the optical gain may also be excitonic (involving bound electron–hole pairs, rather than free charge carriers) in the nitrides. Indeed, unlike in red or infrared lasers where excitons cannot survive at room temperature and under the high injected carrier densities associated with lasing, the optical gain in the nitrides may arise from exciton recombination; or at least the gain is somehow 'Coulomb-enhanced', where the attractive interaction between the electron and hole plasmas becomes important. If the gain is excitonic, even slight InGaN composition variations could be significant, as they would induce weak potential fluctuations in the quantum well plane, leading to exciton localization. These issues remain to be explored fully.

### Applications

The high efficiency and longevity of the III–V nitrides satisfy the requirements for short-wavelength visible LEDs. Red traffic signals are currently produced by filtering the red portion of incandescent lamps, wasting about 85% of the emitted light. To obtain green and amber, nearly 30% of the light must be filtered out. Power efficiency is an important factor for traffic lights, as they typically operate continuously throughout the day. In addition, LEDs have lifetimes of over 5 years whereas incandescent lamps need replacement a few times per year. The combined savings in consumed energy and in replacement costs make the use of LEDs in traffic signals economically desirable.

Large full-colour outdoor electroluminescent displays using green and blue InGaN LEDs already exist in various cities, and more are expected as the relatively large cost is compensated by their impact. Automobile interior panel lighting is also an important market for full-colour LEDs. As manufacturing costs drop with increased mass production, similar considerations will apply to all types of lighting: home and office lighting might also be generated by LEDs, installed as permanent fixtures to last the lifetime of the building.

Short-wavelength injection lasers are highly desirable for applications such as ultra-high-density optical data storage, high-resolution printing, and for defence-related underwater communications

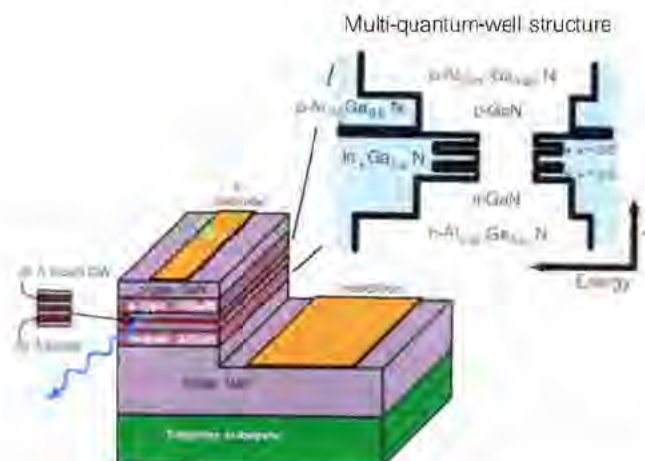


**Figure 7** Diagram of the structure of InGaN multiple quantum well (MQW) diode laser<sup>47</sup>. Inset shows the energy band diagram associated with the MQW structure. Carrier confinement is achieved by the adjacent layers of wider bandgap GaN

and the AlGaN cladding layers. In addition, the p-type  $\text{Al}_{0.2}\text{Ga}_{0.8}\text{N}$  layer immediately above the MQW may play a critical role in carrier confinement.

requiring green lasers. The first of these, optical data storage, is a dominant motivation for blue-laser development. This can be understood by noting that in the diffraction limit, the minimum spot size for a given optical system is proportional to wavelength  $\lambda$ ; thus the optical recording areal densities scale as  $1/\lambda^2$ . Furthermore, as the data are more tightly stored on such a disk, the data retrieval rate is also increased. Current optical disks are based on infrared light ( $\lambda = 780$  nm) and are in the process of upgrading to red light ( $\lambda = 650$  nm). With the recent demonstrations of blue laser diodes ( $\lambda = 450$  nm), it seems that the commercial prospects are promising, particularly for digital video disk technology. The figure of merit of data-storage technologies is the areal density; currently, commercial devices offer  $500 \text{ Mbit in}^{-2}$ . With the advent of blue lasers, this figure will be increased by a factor of four as a result of the shorter wavelength. Similar considerations also apply to high-resolution printers, where a small focused spot translates into greater resolution. Other applications on the horizon include full-colour film printers, projection television and biomedical uses.

## Challenges

Perhaps the main challenge in the field of the nitrides is to increase the lifetime of diode lasers operating at room temperature. The short lifetimes are caused by heating during operation, a consequence of the high threshold current along with the relatively high electrical resistance of nitride lasers. The heating problem may therefore be ameliorated either by reducing the threshold current or by lessening the diode's electrical resistance. Although theories indicate that the threshold currents are relatively high for the nitrides (higher than for red or infrared lasers), it is difficult to assess how this depends on the highly dislocated crystal structure. For example, defects may be responsible for other recombination pathways, or they may scatter light out of the optical cavity. Better lattice-matched substrates might lower thresholds by eliminating crystal defects; but on the other hand, the fact that nitride LEDs already show high quantum efficiencies despite their high dislocation densities may indicate that dislocations are not seriously detrimental (although scattering is not a problem in LEDs, it is a serious issue in lasers). In fact, dislocations can under certain conditions actually be favourable, as they may provide mechanisms by which thermal strain is relieved.

Reducing the electrical resistance of nitride laser diodes would similarly bring closer the goal of reliable, continuous, room-temperature operation. At present, the nitride diodes are relatively resistive, leading to severe heating at the high current densities required of lasing. Of the many component layers making up the diode, the metal contact to the p-type layers is especially resistive, usually dominating the total series resistance of the diode. This is so because of the limited p-type doping possible in the nitrides, and the high Schottky energy barrier associated with the interface between a metal and a high-bandgap semiconductor. Energy conservation requires that in order to support injection, the diode voltage should be at least equal to the photon energy divided by the electronic charge, corresponding to about 3 V for a 420 nm violet photon. In red and infrared laser diodes, the diode voltage at threshold is typically a few tenths of a volt above this. In contrast, the diode voltage of the first nitride laser was about 35 V. This included the drop of  $\sim 3$  V across the p-n junction, and the remaining  $\sim 30$  V across the metal-semiconductor contact. Reducing the p-contact resistance, either by higher doping or alternative contact materials, is therefore critical to overcoming the heating problem sufficiently to obtain long-lived continuous operation of nitride lasers at room temperature.

Spanning a broader range of wavelengths is also an aim of nitride laser development, driven by numerous potential applications. For example, communication through sea water is performed optimally at green wavelengths ( $\sim 505$  nm), whereas optical data storage demands as short a wavelength as possible while remaining con-

sistent with the spectral range over which inexpensive optical systems maintain their transparency.

Expanding nitride laser operation from the ultraviolet or violet to longer wavelengths is made challenging primarily by the growth of high-indium-content InGa<sub>N</sub> alloys for the active region. In principle, the composition of an InGa<sub>N</sub> alloy active region can be adjusted to give emission throughout the entire visible spectrum. For instance, a thin (20–50 Å) In<sub>0.3</sub>Ga<sub>0.7</sub>N layer provides blue emission, whereas increasing the indium content from 30 to 50% shifts the wavelength to green. However, because the lattice parameter of InGa<sub>N</sub> alloys is larger than for GaN, only thin layers can be grown before structural defects such as dislocations or alloy segregation (where the strain within a uniform InGa<sub>N</sub> alloy film causes it to dissociate into regions of highly disparate compositions) arise. These limitations of InGa<sub>N</sub> growth are still being investigated.

With the advent of the nitride-based semiconductors, the long search for bright solid-state sources covering the full range of the visible spectrum seems to be over. Green and blue nitride light-emitting diodes are now available commercially with surprisingly high efficiencies and long lifetimes. Blue and ultraviolet diode lasers have been demonstrated under pulsed conditions, and continuous operation of nitride lasers for tens of hours is already possible. These exciting recent developments have been made possible only by decades of persistent research, and by the unique characteristics of the nitride-based semiconductors. They promise a bright future for photonic technology. □

F. A. Ponce and D. P. Bour are at Xerox Palo Alto Research Center, 3333 Coyote Hill Road, Palo Alto, California 94304, USA.

1. Lighting and lighting devices in *The New Encyclopedia Britannica* 15th Edn, Vol. 23, 29–38 (Encyclopaedia Britannica Inc., Chicago, 1986).
2. Black, J., Lowcockwood, H. & Mayburg, S. Recombination radiation in GaAs. *J. Appl. Phys.* **34**, 178–180 (1963).
3. Holonyak, H. Jr & Bevacqua, S. F. Coherent (visible) light emission from Ga(As<sub>1-x</sub>P<sub>x</sub>) junctions. *Appl. Phys. Lett.* **1**, 82–83 (1962).
4. Dupuis, R. D. An introduction to the development of the semiconductor laser. *IEEE J. Quant. Electr.* **QE-23**, 651–657 (1987).
5. Craford, M. G. LEDs challenge the incandescents. *IEEE Circuit Devices* **8**, 25–29 (1992).
6. Craford, M. G. & Steranka, F. M. Light Emitting Diodes, in *Encyclopedia of Applied Physics* Vol. 8, 485–514 (VCH, New York, 1994).
7. Akasaki, I. & Amano, H. Wide-gap column-III nitride semiconductors for UV/blue light emitting devices. *J. Electrochem. Soc.* **141**, 2266–2271 (1994).
8. Morkoc, H. et al. Large-band-gap SiC, III-V nitride, and II-VI ZnSe-based semiconductor device technologies. *J. Appl. Phys.* **76**, 1363–1398 (1994).
9. Mohammad, S. N., Salvador, A. A. & Morkoc, H. Emerging gallium nitride based devices. *Proc. IEEE* **83**, 1306–1355 (1995).
10. Neumayer, D. A. & Ekerdt, J. G. Growth of group III nitrides: A review of precursors and techniques. *Chem. Mater.* **8**, 9–25 (1996).
11. Nakamura, S. et al. InGa<sub>N</sub>-based multi-quantum-well structure laser diodes. *Jpn. J. Appl. Phys.* **35**, L74–L76 (1996).
12. Nakamura, S. Characteristics of InGa<sub>N</sub> multi-quantum-well-structure laser diodes. *Mater. Res. Soc. Proc.* **449**, 1135–1142 (1996).
13. Kuo, C. P., Fletcher, R. M., Osentowski, T. D., Lardizabal, M. C. & Craford, M. G. High performance AlGaInP visible light-emitting diodes. *Appl. Phys. Lett.* **57**, 2937–2939 (1990).
14. Fichter, F. Über Aluminiumnitrid. *Z. Anorg. Chem.* **54**, 322–327 (1907).
15. Lirmann, J. V. & Schdanov, H. S. The crystalline structure of GaN. *Acta Physicochim. URSS* **6**, 306 (1937).
16. Maruska, H. P. & Tietjen, J. J. The preparation and properties of vapor-deposited single-crystalline GaN. *Appl. Phys. Lett.* **15**, 327–329 (1969).
17. Pankove, J. L., Miller, E. A. & Berkeyheiser, J. E. GaN electroluminescent diodes. *RCA Rev.* **32**, 383–392 (1971).
18. Manasevit, H. M., Erdmann, F. M. & Simpson, W. I. The use of metalorganics in the preparation of semiconductor materials. *J. Electrochem. Soc.* **118**, 1864–1868 (1971).
19. Dingle, R., Shalke, K. L., Leheny, R. F. & Zetterstrom, R. B. Stimulated emission and laser action in gallium nitride. *Appl. Phys. Lett.* **19**, 5–7 (1971).
20. Yoshida, S., Miawata, S. & Gonda, S. Improvements on the electrical and luminescent properties of reactive molecular beam epitaxially grown GaN films by using AlN-coated sapphire substrates. *Appl. Phys. Lett.* **42**, 427–429 (1983).
21. Chang, C.-A., Takaoka, H., Chang, L. L. & Esaki, L. Molecular beam epitaxy of AlSb. *Appl. Phys. Lett.* **40**, 983–985 (1982).
22. Wang, W. I. Molecular beam epitaxial growth and material properties of GaAs and AlGaAs on Si(100). *Appl. Phys. Lett.* **44**, 1149–1151 (1984).
23. Amano, H., Sawaki, N., Akasaki, I. & Toyoda, Y. Metalorganic vapor phase epitaxial growth of a high quality GaN film using an AlN buffer layer. *Appl. Phys. Lett.* **48**, 353–355 (1986).
24. Johnson, N. M., Burnham, R. D., Street, R. A. & Thornton, R. L. Hydrogen passivation of shallow-acceptor impurities in p-type GaAs. *Phys. Rev. B* **33**, 1102–1105 (1986).
25. Antell, G. R. et al. Passivation of zinc acceptors in InP by atomic hydrogen coming from arsine during metalorganic vapor phase epitaxy. *Appl. Phys. Lett.* **53**, 758–760 (1988).
26. Amano, H., Kito, M., Hiramatsu, K. & Akasaki, I. P-type conduction in Mg-doped GaN treated with low-energy electron beam irradiation (LEEBI). *Jpn. J. Appl. Phys.* **28**, L2112–L2114 (1989).
27. Nakamura, S., Mukai, T., Senoh, M. & Iwasa, N. Thermal annealing effects on p-type Mg-doped GaN films. *Jpn. J. Appl. Phys.* **31**, L139–L142 (1992).



28. Akasaki, I., Amano, H., Itoh, K., Koide, N. & Manabe, K. GaN-based ultraviolet/blue light emitting devices. *Inst. Phys. Conf. Ser.* **129**, 851–856 (1992).
29. Nakamura, S., Mukai, T., Senoh, M., Nagahama, S. & Iwasa, N. InGa<sub>1-x</sub>N/InGa<sub>1-x</sub>N superlattices grown on GaN films. *J. Appl. Phys.* **74**, 3911–3915 (1993).
30. Nakamura, S., Mukai, T. & Senoh, M. Candela-class high-brightness InGaN/AlGa<sub>x</sub>N double-heterostructure blue-light-emitting diodes. *Appl. Phys. Lett.* **64**, 1687–1689 (1994).
31. Nakamura, S., Mukai, T. & Senoh, M. High-brightness InGaN/AlGa<sub>x</sub>N double heterostructure blue-green light-emitting diodes. *J. Appl. Phys.* **76**, 8189–8191 (1994).
32. Lester, S. D., Ponce, F. A., Craford, M. G. & Steigerwald, D. A. High dislocation densities in high efficiency GaN-based light-emitting diodes. *Appl. Phys. Lett.* **66**, 1249–1251 (1995).
33. Nakamura, S., Senoh, M., Iwasa, N. & Nagahama, S. High-brightness InGa<sub>x</sub>N blue, green and yellow light-emitting diodes with quantum well structures. *Jpn. J. Appl. Phys.* **34**, L797–L799 (1995).
34. Nakamura, S., Senoh, M., Iwasa, N., Nagahama, S., Yamada T. & Mukai, T. Superbright green InGa<sub>x</sub>N SQW structure LEDs. *Jpn. J. Appl. Phys.* **34**, L1332–L1335 (1995).
35. Ponce, F. A., Major, J. S. Jr, Plano, W. E. & Welch, D. F. Crystalline structure of AlGa<sub>x</sub>N epitaxy on sapphire using AlN buffer layers. *Appl. Phys. Lett.* **65**, 2302–2304 (1994).
36. Ponce, F. A., Bour, D. P., Götz, W. & Wright, P. J. Spatial distribution of the luminescence in GaN thin films. *Appl. Phys. Lett.* **68**, 57–59 (1996).
37. Nakamura, S. GaN growth using GaN buffer layer. *Jpn. J. Appl. Phys.* **30**, L1705–L1707 (1991).
38. Ponce, F. A., Krusor, B. S., Major, J. S. Jr, Plano, W. E. & Welch, D. F. Microstructure of GaN epitaxy on SiC using AlN buffer layers. *Appl. Phys. Lett.* **67**, 410–412 (1995).
39. Ponce, F. A., Van de Walle, C. G. & Northrup, J. E. Atomic arrangement at the AlN/SiC interface. *Phys. Rev. B* **53**, 7473–7478 (1996).
40. Ponce, F. A. *et al.* Homoepitaxy of GaN on polished bulk single crystals by metalorganic chemical vapor deposition. *Appl. Phys. Lett.* **68**, 917–919 (1996).
41. Amano, H., Asahi, T. & Akasaki, I. Stimulated emission near ultraviolet at room temperature from a GaN film grown on sapphire by MOVPE using an AlN buffer layer. *Jpn. J. Appl. Phys.* **29**, L205–L206 (1990).
42. Zubrilov, A. S. *et al.* Spontaneous and stimulated emission from photopumped GaN grown on SiC. *Appl. Phys. Lett.* **67**, 533–535 (1995).
43. Khan, M. A., Krishnakutty, S., Skogman, R. A., Kuznia, J. N. & Olson, D. T. Vertical-cavity stimulated emission from photopumped InGa<sub>x</sub>N/GaN heterojunctions at room temperature. *Appl. Phys. Lett.* **65**, 520–521 (1994).
44. Kim, S. T., Amano, H. & Akasaki, I. Surface-mode stimulated emission from optically pumped GaInN at room temperature. *Appl. Phys. Lett.* **67**, 267–269 (1995).
45. Amano, H. *et al.* Room-temperature violet stimulated emission from optically pumped AlGa<sub>x</sub>N/GaInN double heterostructure. *Appl. Phys. Lett.* **64**, 1377–1379 (1994).
46. Aggarwal, R. L., Maki, P. A., Molnar, R. J., Liao, Z.-L. & McInnis, I. Optically pumped GaN/AlGa<sub>x</sub>N double heterostructure ultraviolet laser. *J. Appl. Phys.* **79**, 2148–2150 (1996).
47. Nakamura, S. *et al.* InGa<sub>x</sub>N multi-quantum-well-structure laser diodes with cleaved mirror cavity facets. *Jpn. J. Appl. Phys.* **35**, L217–L219 (1996).
48. Nakamura, S. *et al.* Ridge-geometry InGa<sub>x</sub>N multi-quantum-well-structure laser diodes. *Appl. Phys. Lett.* **69**, 1477–1479 (1996).
49. Akasaki, I. *et al.* Shortest wavelength semiconductor laser diode. *Electron. Lett.* **32**, 1105–1106 (1996).
50. Itaya, K. *et al.* Room temperature pulsed operation of nitride based multi-quantum-well laser diodes with cleaved facets on conventional c-face sapphire substrates. *Jpn. J. Appl. Phys.* **35**, L1315–L1317 (1996).
51. Matsumoto T. & Aoki, M. Temperature dependence of photoluminescence from GaN. *Jpn. J. Appl. Phys.* **13**, 1804–1807 (1974).
52. Akasaki, I. & Hayashi, I. Research on blue emitting devices. *Ind. Sci. Technol.* **17**, 48–52 (1976) (in Japanese).
53. Yoshida, S., Misawa, S. & Itoh, A. Epitaxial growth of aluminum nitride films on sapphire by reactive evaporation. *Appl. Phys. Lett.* **26**, 461–462 (1975).
54. Karpinski, J., Porowski, S. & Miotkowska, S. High pressure vapor growth of GaN. *J. Cryst. Growth* **56**, 77–82 (1982).
55. Nagamoto, T., Kuboyama, T., Minamino, H. & Omoto, O. Properties of Ga<sub>1-x</sub>In<sub>x</sub>N films prepared by MOVPE. *Jpn. J. Appl. Phys.* **28**, L1334–L1336 (1989).
56. Nakamura, S. & Mukai, T. High-quality InGa<sub>x</sub>N films grown on GaN films. *Jpn. J. Appl. Phys.* **31**, L1457–L1459 (1992).
57. Hunt, R. W. G. *Measuring Colour* 1–313 (Ellis Horwood, London, 1995).
58. Wicks, G. W. The colour of light. *Compound Semiconductor* **1**, 39–40 (1995).

**Acknowledgements.** We acknowledge partial support from the Department of Commerce Advanced Technology Program, and from ARPA.

Correspondence should be addressed to F.A.P. (e-mail: ponce@parc.xerox.com).